UNIVERSITÀ CATTOLICA del Sacro Cuore

DIPARTIMENTO DI SCIENZE ECONOMICHE E SOCIALI

A Duopoly Cournot Model with delayed Expectations

Fernando Bignami
Anna Agliari

Quaderno n. 127/agosto 2017

VP VITA E PENSIERO

Università Cattolica del Sacro Cuore

DIPARTIMENTO DI SCIENZE ECONOMICHE E SOCIALI

A Duopoly Cournot Model with delayed Expectations

Fernando Bignami
Anna Agliari

Quaderno n. 127/agosto 2017

VP VITA E PENSIERO

Fernando Bignami, Dipartimento di Scienze Economiche e Sociali, Università Cattolica del Sacro Cuore, Piacenza (corresponding author).

Anna Agliari, Dipartimento di Scienze Economiche e Sociali, Università Cattolica del Sacro Cuore, Piacenza.

fernando.bignami@unicatt.it

anna.agliari@unicatt.it

I quaderni possono essere richiesti a:
Dipartimento di Scienze Economiche e Sociali,
Università Cattolica del Sacro Cuore
Via Emilia Parmense 84 - 29122 Piacenza - Tel. 0523 599.342
http://dipartimenti.unicatt.it/dises

dises-pc@unicatt.it

www.vitaepensiero.it

ISBN 978-88-343-3434-8

Abstract

We consider a Cournot duopoly with isoelastic demand function and constant marginal costs. We assume that both producers have naive expectations but one of them reacts with delay to the move of its competitors, due to a "less efficient" production process of a competitor with respect to its opponent. The model is described by a 3D map having the so-called "cube separate property", that is its third iterate has separate components. We show that many cycles may coexist and, through global analysis, we characterize their basins of attraction. We also study t he chaotic dynamics generated by the model, howing that the attracting set is either a parallelepiped or the union of coexisting parallelepipeds. We also prove that such attracting sets coexist with chaotic surfaces, having the shape of generalized cylinders, and with different chaotic curves.

1 Introduction

In 2000, Bischi, Gardini and Mammana [5] have studied a class of two-dimensional discrete maps having the property that their second iterate is a decoupled map. The essential result of such a study is that the dynamic properties of this kind of maps can be deduced from the simple analysis of a components of their second iterate, a one-dimensional map. More recently, Agliari, Fournier-Prunaret and Taha [4] have obtained analogous results considering a three-dimensional family of maps having third iterate with separate components. A typical feature of such maps is the coexistence of many invariant orbits, so that multistability situations are recurring. In the 3D case, for example, it is sufficient that the 1D map has a cycle of period 2 to obtain two coexisting cycles for the starting map. And the same holds when chaotic dynamics are involved.

During the last years, many applications to Cournot duopoly have been studied, considering the quantity adjustment over time based on a two-dimensional map with separate second iterate (see, among others, [12], [5], [13]). Indeed "square separate maps" naturally arise when producers have naive expectations.

In the present paper, we consider a Cournot model in which producers have naive expectations about the production of the competitor, but one of them reacts with delay to the move of its competitor. From an economic point of view such an assumption can be justified by the fact that one of two competitors has a "slower" production process, meaning that its production process is technologically less advanced and consequently requires a longer time to react to the market demand. Stated in other words, we can say that a competitor has a production process "less efficient" that its opponent.

Recently many authors have studied Cournot duopoly model with delay; in particular they have considered markets with memory, that is the expected quantity is a weighted average of the past quantity observations (see for example [6], [7], [14]). Here the framework is completely different, since we focus on the "delayed production" of a competitor.

The model under scrutiny is described by a discrete 2D *time-delayed system*, that can be rewrite as a 3D map M with the "cubic separate property", that is, its third iterate has separated components. Our aim is to perform a global analysis of the model, characterizing the basin of attractions of the different coexisting attractors. Moreover, we shall extend the results in [4], deepening the study of the chaotic attractors of M. In particular, we shall analytically show that the three-dimensional chaotic sets (parallelepipeds) coexist with chaotic surfaces, given by union of generalized cylinders, and with chaotic curves.

The rest of the paper is organized as follows. In Section 2 we introduce the model describing the time evolution of the production levels of the two firms. We obtain a 3D map having third iterate with separate components. Then, for convenience of the reader, we recall some results achieved by Agliari et al. (see [4]) related to this kind of maps. In Section 3 we show that the model exhibits multiplicity of cycles and characterize their basins of attraction. In Section 4, extending the results of [4], we study the chaotic attractors (parallelepileds), showing that they coexist with many chaotic surfaces and curves. Section 5 concludes.

2 The model

We consider a Cournot duopoly in which two competitors produce perfect substitute goods. Following Puu [12], we assume an isoelastic demand function and constant marginal costs. Denoting by x and y the supplies of the competitors, the profits are given by

$$\Pi_1 = \frac{x}{x+y} - ax, \qquad \Pi_2 = \frac{y}{x+y} - by$$

where a and b are the constant marginal costs and, consequently, positive parameters.

The *Cournot-Nash reaction functions* of the two firms depend on the expected production of the opponent and are given by:

$$\begin{aligned} r_1\left(y^{(e)}\right) &= \arg\max_x \Pi_1\left(x, y^{(e)}\right) = \sqrt{\frac{y^{(e)}}{a}} - y^{(e)} \\ r_2\left(x^{(e)}\right) &= \arg\max_y \Pi_2\left(x^{(e)}, y\right) = \sqrt{\frac{x^{(e)}}{b}} - x^{(e)} \end{aligned} \tag{1}$$

defined in $\mathbb{R}_+$.

We conjecture that the firms adopt a "learning by doing" approach. Then in the time evolution of the production decisions, we assume that at each stage firms optimally decide following their reaction function, supposing that the production of the opponent remains the same. This means that the firms have *naive expectations.* Furthermore, we assume that a producer reacts with *delay* to the move of its opponent:

$$q_{1,t}^{(e)} = q_{2,t-1} \text{ and } q_{2,t}^{(e)} = q_{1,t-2}$$

In this way we obtain a discrete two dimensional *time-delayed system:*

$$\begin{cases} x_{t+1} = \sqrt{\frac{y_t}{a}} - y_t \\ y_{t+1} = \sqrt{\frac{x_{t-1}}{b}} - x_{t-1} \end{cases} \tag{2}$$

By means of an auxiliary variable z, we can rewrite (2) as a three dimensional model:

$$T : \begin{cases} x' = \sqrt{\frac{y}{a}} - y \\ y' = \sqrt{\frac{z}{b}} - z \\ z' = x \end{cases} \tag{3}$$

where the symbol ' denotes the unit time advancement operator, that is, if (x, y, z) represents the vector of choiches at time t, then (x', y', z') gives the choiches at time $t+1$.

It is easy to see that the map (3) is not defined in the whole three dimensional phase-space. In fact the domain of T is the region D given by:

$$D = \{(x, y, z) : \; y \geq 0, \, z \geq 0\}$$

We are interested in a subset of D, denoted by S, which consists in the points (x, y, z) for which we have $T^n(x, y, z) \in D$, for any $n \geq 0$. We shall call *admissible* such points and trajectories in S:

$$S = \{(x, y, z) \in D : T^n(x, y, z) \in D \; \forall n \geq 0\} .$$

Before to start the analysis of the map (3) in the phase-space D we show that the two marginal costs (a, b) are redundant parameters. This follows from the observation that the maps T with parameters (a, b) and $\widetilde{T}$ with parameters $(\tau a, \tau b)$ with $\tau > 0$ are *topologically conjugate* via the homeomorphism $\Phi(x, y, z) = (\tau x, \tau y, \tau z)$, being $T = \Phi \circ \widetilde{T} \circ \Phi^{-1}$ or, equivalently, $\widetilde{T} = \Phi^{-1} \circ T \circ \Phi$. In the present model we have:

$$\widetilde{T} : \begin{cases} x' = \sqrt{\frac{y}{\tau a}} - y \\ y' = \sqrt{\frac{z}{\tau b}} - z \\ z' = x \end{cases}$$

Considering $\tau = \frac{1}{a}$ and setting $k = \frac{b}{a}$, we obtain the map:

$$M : \begin{cases} x' = \sqrt{y} - y \\ y' = \sqrt{\frac{z}{k}} - z \\ z' = x \end{cases} \tag{4}$$

Due to topological conjugacy, the dynamics of the map T which depends on two parameters (a, b) and the dynamics of the map M which depends on a unique parameter, k, have the same qualitative behaviour, because they are associated by a simple coordinate transformation (see, [2]). In other words, through the topological conjugacy we have obtained a *reduction* in the number of parameters of the map T in (3), since only the ratio between marginal costs has to be considered.

Henceforth, we take the analysis considering the map M in (4) and $k \in (0, 1]$, assuming that producer 1 has higher marginal costs than its competitor. From an economic point of view, this choice can be motivated by the fact that producer 2 claims lower costs having a production process "less efficient" than its competitor, which causes delayed reaction to the moves of its opponent.

2.1 Properties of "cube separate maps"

Related to the aim of the present paper, the fundamental property of the map M in (4) is that *its third forward iterate has separate components,* which we will call "*cube separate property*". Indeed the map in (4) belongs to the particular class of maps:

$$\Psi : \begin{cases} x' = f(y) \\ y' = g(z) \\ z' = h(x) \end{cases} \tag{5}$$

and $\Psi^{3n}(x, y, z) = (H^n(x), F^n(y), G^n(z))$, for each integer $n \geq 0$, with $H(x) = f(g(h(x)))$, $F(y) = g(h(f(y)))$, $G(z) = h(f(g(z)))$ and F^0, G^0, H^0 identity functions.

The family of map (5) has been studied by Agliari et al. (see, [4], [3]) and, for convenience of the reader, we recall here some results, useful for the understanding of the subsequent analysis of the model. These results are based on the following relationships: for any $n \geq 1$ the three one dimensional (1D) maps H, F and G satisfy:

- $h \circ H^n(x) = G^n \circ h(x)$
- $g \circ G^n(z) = F^n \circ g(z)$
- $f \circ F^n(y) = H^n \circ f(y)$

and

- $g \circ h \circ H^n(x) = F^n \circ g \circ h(x)$
- $f \circ g \circ G^n(z) = H^n \circ f \circ g(z)$
- $h \circ f \circ F^n(y) = G^n \circ h \circ f(y)$.

Such properties imply that the invariant sets of the 1D maps H, G and F are strictly correlated. As an example, we have that any $n-$cycle of the map H, $\{x_1, x_2, ..., x_n\}$ admits *conjugated cycles*, given by a $n-$cycle of the map G, i.e. $\{z_1, z_2, ..., z_n\} =$

$\{h(x_1), h(x_2), ..., h(x_n)\}$, and a $n-$cycle of the map F, i.e. $\{y_1, y_2, ..., y_n\} = \{g(h(x_1)), ..., g(h(x_n))\}$ [1]. We remark that conjugated cycles have all the same stability property, since their multipliers are equal.

In the following we shall consider the map H to study the attractors of Ψ as well as their stability properties.

As shown in [4], a correspondence exists between the cycles of the 3D map Ψ and those of H. Indeed (x, y, z) is a periodic point of a n-cycle of Ψ iff x is a periodic points of a cycle of H

- either of prime period $\frac{n}{3}$ or a divisor of $\frac{n}{3}$, when n is a multiple of 3, and y, z are periodic points of F and G
- of the same prime period n, otherwise, and y, z belongs to the conjugated cycles of F and G.

A consequence is that the set $\mathcal{P}$ of the periodic poins of the map Ψ is given by:

$$\mathcal{P} = \mathcal{X} \times \mathcal{Y} \times \mathcal{Z} \tag{6}$$

where $\mathcal{X}$, $\mathcal{Y}$ and $\mathcal{Z}$ are the sets of periodic points of the one dimensional maps H, F and G.

The cycles of Ψ can be generated starting either by a unique cycle or by periodic points belonging to different coexisting cycles of H.

Definition 1 *A cycle of the three dimensional map Ψ is said homogeneous if the components of its periodic points belong to conjugate cycles of H, F and G. Otherwise, it is called mixed cycle.*

Remark that all cycles of Ψ having a period not multiple of 3 are homogeneous, while those having a period multiple of 3 can be either homogeneous or mixed cycles.

More precisely, considering a single cycle of H of period n we can obtain that

[1] Obviously, the same result holds starting from a cycle of G (or F).

- *if* $n = 3s+1$ or $n = 3s+2$ then Ψ has 1 homogeneous cycles of period n and $\frac{n^2-1}{3}$ homogeneous cycles of period $3n$;

- if $n = 3s$ then Ψ has $\frac{n^2}{3}$ homogeneous cycles of period $3n$.

It is worth to observe that if $n > 1$ then the map Ψ exibits coexistence of cycles.

Furthermore, if the map H admits coexisting cycles then, besides the homogeneous cycles associated with each one of the cycles of H, the map Ψ has further cycles, whose periodic points are given by the mixing of the periodic points of different cycles, that is of mixed type.

Any pair of coexisting cycles of the map H, of period n and m, generate $(n+m)\frac{nm}{s}$ different mixed cycles of period $3s$ of the map Ψ, being $s = LCM\,(m,n)$, where LCM means the last common multiple.

Any triplet of coexisting cycles of the map H, of period n, m and p, generate $2\frac{nmp}{S}$ different mixed cycles of period $3S$ of the map Ψ, besides the homogeneous ones and those generated by any pair of the three cycles of H. Here $S = LCM\,(n,m,p)$.

We refer to [4] to identify the single homogeneous and mixed cycles so obtained, and we conclude recalling how the local stability of the different cycles can be inferred.

Starting from a n-cycle of the 1D map H with eigenvalue λ, all the homogeneous cycles of the 3D map Ψ of period $3n$ have equal eigenvalues $\lambda_1 = \lambda_2 = \lambda_3 = \lambda$, while the homogeneous cycles of Ψ of period n, when n is not a multiple of 3, have eigenvalues $\lambda_1 = \sqrt[3]{\lambda}$, $\lambda_2 = \sqrt[3]{\lambda}\left(-\frac{1}{2} - \frac{\sqrt{3}}{2}i\right)$ and $\lambda_3 = \sqrt[3]{\lambda}\left(-\frac{1}{2} + \frac{\sqrt{3}}{2}i\right)$. This means that stable (unstable) cycles of H give rise to stable (unstable) homogeneous cycles of Ψ. Moreover, any local bifurcation of a cycle of the map H corresponds to a local bifurcation of $3D$ map at which three eigenvalues cross simultaneously the unit circle (that is, the local bifurcations of the Ψ map is of *co-dimension* 3).

Regarding the mixed cycles, we can say that when the map H has three coexisting cycles $X = \{x_i\}$, $A = \{\alpha_j\}$ and $\Delta = \{\delta_l\}$ with eigenvalues λ_x, λ_α and λ_δ respectively, then the mixed cycles of the three-dimensional map Ψ generated by two coexisting cycles of H, say X and A, have eigenvalues either $(\lambda_x, \lambda_x, \lambda_\alpha)$ or $(\lambda_x, \lambda_\alpha, \lambda_\alpha)$, depending on the number of their components belonging to X and its conjugates. The mixed cycles of the three-dimensional map Ψ generated by the three coexisting cycles of H have eigenvalues $(\lambda_x, \lambda_\delta, \lambda_\delta)$ (for major details see [4]).

3 Coexisting cycles for the map M

The aim of the present paper is to investigate the attracting sets of the map M and their basins of attractions. As it is well known the basin of an attractor $\mathcal{A}$ is defined as (see [1])

$$\mathcal{B}(\mathcal{A}) = \cup_{n=0}^{\infty} M^{-n}(U(\mathcal{A}))$$

where $M^{-n}(P)$ represent the set of the rank$-n$ preimages of P and $U(\mathcal{A})$ is a neighbourhood of $\mathcal{A}$ whose trajectories converge to A. Then, it is clear that the invertibility/noninvertibility property of M is very important in order to understand the structure of the basins and their bifurcations. Indeed, when a map is noninvertible the basins of attraction may have different structures (connected, multiply connected, disconnected or even more complex), see, for instance, [11]. For that reason, we start our analysis from the study of the *Riemann foliation* of the space $\mathbb{R}^3_+$ associated with M (see, [9], [8]).

We recall that a map M is noninvertible if, given a point $p \in S$, the *rank-1 preimage* of p' (that is, the point p such that $p' = M(p)$) may not exist or may be not unique. In other words, a noninvertible map is a correspondence many-to-one, that is distinct points of the space may have the same forward image and points without preimages may exist (see [8]).

It is easy to see that M is a noninvertible map. Indeed, the rank-1 preimages of a given point $(u, v, w) \in \mathbb{R}^3_+$ are the solutions of the algebraic system

$$\left\{\begin{array}{c} u=\sqrt{y}-y \\ v=\sqrt{\frac{z}{k}}-z \\ w=x \end{array}\right. \tag{7}$$

in the unknow variables (x, y, z). System (7) admits four solutions iff $0 \leq u \leq \frac{1}{4}$ and $0 \leq v \leq \frac{1}{4k}$. They are given by

$$M_1^{-1}:\left\{\begin{array}{c} y=\frac{1-2u-\sqrt{1-4u}}{2} \\ z=\frac{1-2kv-\sqrt{1-4kv}}{2k} \\ x=w \end{array}\right.$$

$$M_2^{-1}:\left\{\begin{array}{c} y=\frac{1-2u-\sqrt{1-4u}}{2} \\ z=\frac{1-2kv+\sqrt{1-4kv}}{2k} \\ x=w \end{array}\right.$$

$$M_3^{-1}:\left\{\begin{array}{c} y=\frac{1-2u+\sqrt{1-4u}}{2} \\ z=\frac{1-2kv-\sqrt{1-4kv}}{2k} \\ x=w \end{array}\right.$$

$$M_4^{-1}:\left\{\begin{array}{c} y=\frac{1-2u+\sqrt{1-4u}}{2} \\ z=\frac{1-2kv+\sqrt{1-4kv}}{2k} \\ x=w \end{array}\right.$$

The noninvertibility of the map M is so proved and its multivalued inverse can be represented as

$$M^{-1}=M_1^{-1}\cup M_2^{-1}\cup M_3^{-1}\cup M_4^{-1}$$

Following the terminology introduced in [9] and [8], we can say that M is a Z_0-Z_4 map, meaning that the space $\mathbb{R}_+^3$ is divided in two regions: one of them contains points having no preimages while the points belonging to the second one have four distinct rank-1 preimages. Such regions, or *zones*, are separated by the critical line LC, locus of points having four merging rank-1 preimages. The direct inspection of M^{-1} allows us to obtain that the critical lines LC are made up by two branches: $LC^a = D\cap\left\{x=\frac{1}{4}\right\}$ and $LC^b = D\cap\left\{y=\frac{1}{4k}\right\}$. We conclude that the region Z_4 is a *cylinder whose cross section is a rectangle.*

3.1 Analysis of the 1D map H

Besides the noninvertibility of M even its "cube separate property" plays an important rôle in the analysis of the long run behavior of the map. Indeed, as we have seen in Sec.2.1, such a property implies that the dynamic behavior of the 3D map M can be derived from the study of one of the components of its third iterate. In particular, we shall consider the map $H(x) = f(g(h(x)))$, given by

$$H(x) = \sqrt{\sqrt{\frac{x}{k}} - x} - \sqrt{\frac{x}{k}} + x. \tag{8}$$

The map H is defined in the interval $I = \left[0, \frac{1}{k}\right]$, with $k \in (0,1]$, and always admits two intersections with the x-axis: the origin $O = 0$ and $C = \frac{1}{k}$. Three critical points of H exist: two maximum points $C^M_{-1,a} = \frac{2-k-2\sqrt{1-k}}{4k}$, $C^M_{-1,b} = \frac{2-k+2\sqrt{1-k}}{4k}$ with equal critical value (in the Julia-Fatou sense) $C^M_a = C^M_b = \frac{1}{4}$ and one minimum point $C^m_{-1} = \frac{1}{4k}$ with critical value $C^m = \frac{2\sqrt{k}-1}{4k}$. The minimum value $C^m = \frac{2\sqrt{k}-1}{4k}$ is negative if $k < \frac{1}{4}$, consequently, in this case two further intersections with the $x-$axis exist: $a = \frac{1-2k-\sqrt{1-4k}}{2k}$ and $b = \frac{1-2k+\sqrt{1-4k}}{2k}$ (see Fig.1). This implies that when $k > k_g = \frac{1}{4}$ the feasible trajectories of H belong to the interval $[O, C]$, while in the case $k < k_g$ the feasible set is disconnected, being equal to $[O, a] \cup [b, C]$. Therefore $k = k_g$ corresponds to a global bifurcation value.

Finally, it is straightforward to verify that the map H admits $x^* = \frac{k}{(1+k)^2}$ as a fixed point, besides the trivial one O (always unstable). The evaluation at x^* of the derivative of the map H allows us to conclude that x^* is stable if $3 - 2\sqrt{2} < k < 3 + 2\sqrt{2}$ and its loss of stability occurs through a flip bifurcation. Since we are considering $k \in (0,1]$, only the bifurcation value $k_f = 3 - 2\sqrt{2}$ has to be considered.

A bifurcation diagram of map H is shown in Fig.2, and we can observe that bounded dynamics exist if $k \geq 0.16$. Indeed, when the bifurcation parameter k decreases from 1, at $k = 3 - 2\sqrt{2}$ a

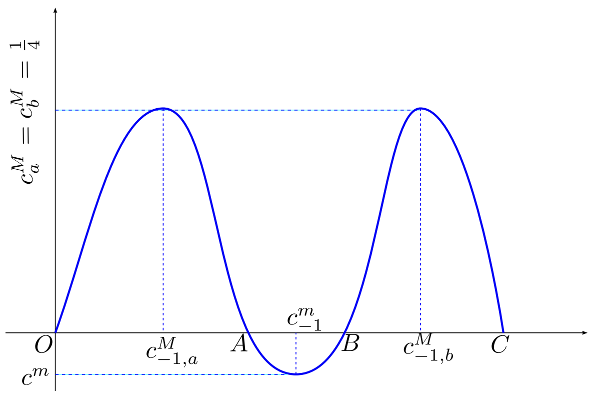

Figure 1: A qualitative draft of the 1D map H when $k < k_g$

supercritical flip bifurcation occurs. Then the usual *Feingenbaum cascade* of period doubling bifurcation takes place and leads to the chaotic behavior of H. At $k = 0.16$ the *final bifurcation* occurs, corresponding to the homoclinic bifurcation of the repelling fixed point. Indeed at $k = 0.16$ the critical point c^M is mapped into the point $(0, 0)$, as it is simple to verify, and the chaotic dynamics of H covers the whole interval $\left[0, C^M\right]$ (*pure chaos*).

3.2 Basin of attraction of the Cournot-Nash equilibrium

Let us come back to the map M. The existence of two fixed points of H implies that also the map M in (4) has two fixed points, the origin O^* and $E^* = (x^*, y^*, x^*)$, where $y^* = g(x^*) = \frac{1}{(1+k)^2}$ as we said in section 2.1. We also know that O^* is unstable, while E^* is stable if $k > k_f$. In order to determine the basin of attraction of E^*, the analysis of the map H suggests that two cases have to be taken into account, depending on the value of the parameter k.

As we have seen, when $k > k_g = frac14$ the feasible set of the map H is a connected set and this also holds for the map M. Indeed, in this case the origin O of $\mathbb{R}^3_+$ has four different rank-1 preimages, O itself and $O^1_{-1}\left(0; 0; \frac{1}{k}\right)$, $O^2_{-1}\left(0; 1; \frac{1}{k}\right)$, $O^3_{-1}\left(0; 1; 0\right)$.

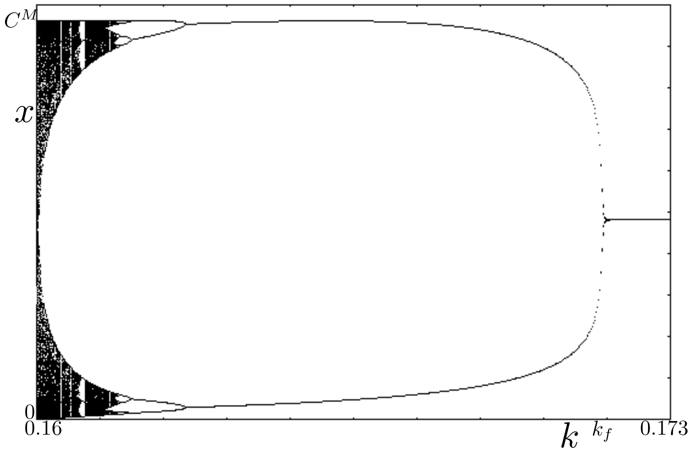

Figure 2: Bifurcation diagram of the map H

Only O^2_{-1} belongs to Z_4 and then only further four rank-2 preimages of O exist, all belonging to Z_0. These preimages are the vertex of a box $\mathcal{B}$ that contains all the bounded trajectories of M (a qualitative draft is given in Fig.3a). Fig.3b confirms that the *rectangular parallelepiped* $\mathcal{B}$ is the basin of attraction of E^*, always stable if $k_g < k < 1$. In particular, Fig.3b shows two cross sections of the connected basin of attraction of E^*. More precisely, one with the plane $z = \frac{1}{k}$, that is the plane through the maximum point of H and one with $z = z^*$ that is the plane that get through the fixed point $E^\star$. Besides the homogeneous cycles (fixed points), the map M exhibits two saddle cycles of period 3, S_1 and S_2, of mixed type, given by

$$S_1 = \{(0^*, y^*, 0^*), (x^*, 0^*, 0^*), (0^*, 0^*, z^*)\}$$
$$S_2 = \{(0^*, y^*, z^*), (x^*, y^*, 0^*), (x^*, 0^*, z^*)\}.$$

In Fig.3a the mutual positions of the coexisting cycles of the map M are represented, as well as the stable and unstable sets of the two saddle cycles. The projection of the two branches of the curve

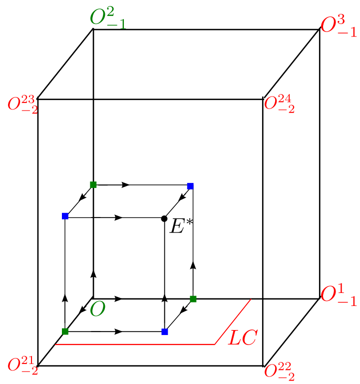

(a) Qualitative draft of $\mathcal{B}$. The squares denote the saddle cycles

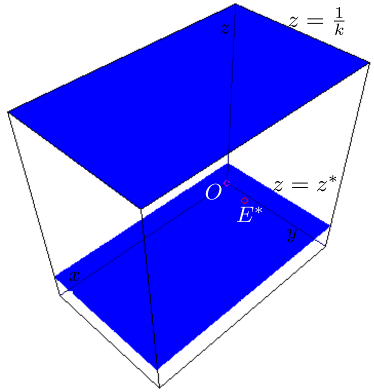

(b) Two sections of the basin of attraction of E^*

Figure 3: The connected basin of attraction of E^* when $k > \frac{1}{4}$

LC are also represented in the same figure, to give an idea of the Z_4 region.

A completely different situation can be observed when $k < k_g$ and the minimum point of the map H has a negative critical value, so that two further preimages of the repelling fixed point O exist, $x = a$ and $x = b$. As we said, in this case a global bifurcation of the map H has occurred and this has also caused an important qualitative change in the basin of attraction of E^*. Indeed, as shown in Fig.4a, all the four preimages of rank-1 of O^* have further preimages and even its preimages of rank-2 may have further preimages. This implies the transition from a connected basin of attraction into a disconnected one. In Fig.4b five cross sections of the basin of attraction of E^* are represented; in particular the two sections $z = a$, $z = b$ are the lower and upper bounds of a portion of the unfeasible set. A further portion of the unfeasible set is bounded by the planes $x = a$ and $x = b$. Concluding, we can say that the basin of attraction of E^* is made up by four components, bounded by planes parallel to the coordinate planes xy and yz

and passing through the preimages of 0 obtained with the map H. Such a structure of the basin of attraction will persist as k further decreases, associated with the attracting set containing all the attractors of the map M.

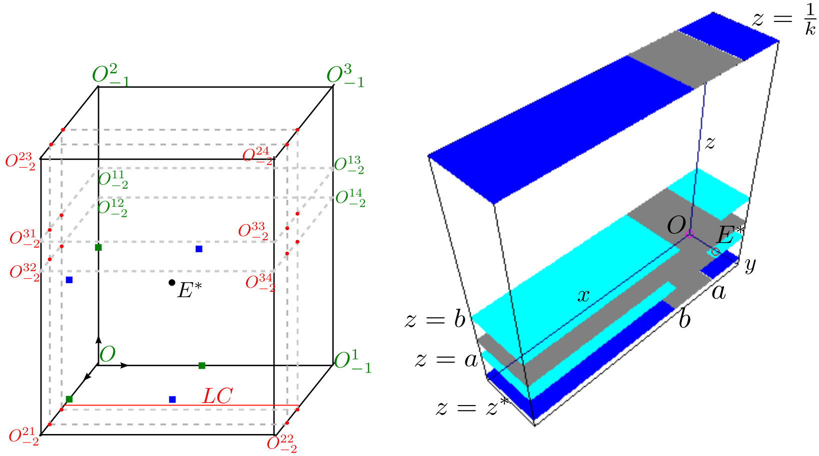

(a) Qualitative draft (b) Sections

Figure 4: Disconnected basin of attraction of E^*

3.3 Coexistence of two stable cycles

Now, we consider $k < k_f$, when E^* becomes unstable. We know that when $k = k_f = 3 - 2\sqrt{2}$ the fixed point x^* of the 1D map H undergoes a *period doubling bifurcation* and immediately after the bifurcation a stable cycle $C = (c_1, c_2)$ of period 2 appears. Bearing in mind section 2.1, we have that the occurrence of the period doubling bifurcation of the fixed point x^* of the map H has important consequences on the map M, since it causes the sudden appearance of 10 cycles, besides the 4 already existing. In particular, we obtain that the map M admits:

A1) two homogeneous stable cycles: one of period 2, C, and one of period 6, D;

A2) four repelling cycles: the two fixed points O^* and E^* (homogeneous) and two mixed cycles of period 3 (mixed);

A3) eight saddles cycles of period 6 of mixed type.

The repelling cycles in A2) have been described above, being due to the existence of the two fixed points of the map H. In order to obtain the periodic points of the new homogeneous cycles, in A1), we recall that if $(a_1, ..., a_n)$ is a cycle of $H(x)$ then $(g(a_1), ...g(a_n))$ is the conjugate cycle of $F(y)$ as well as $(h(a_1), ..., h(a_n)) = (a_1, ..., a_n)$ is the conjugate cycle of $G(z)$. Hence we obtain that the periodic points of the stable cycle of period 2 are given by $\{(c_1, g(c_1), c_2), (c_2, g(c_2), c_1)\}$, while the remaining points of the set $\mathcal{P} = \{c_1, c_2\} \times \{g(c_1), g(c_2)\} \times \{c_1, c_2\}$ belong to the stable cycle of period 6.

Regarding the mixed cycles in A3), we have to consider the coexistence of the cycle C with the fixed points O^* and $x^\star$. We obtain that, being $g(0) = 0$ and $g(x^*) = y^*$

B1) three saddle cycles of period 6 exist, due to the coexistence of C and $O^\star$; they can be obtained starting from the periodic points $(c_1, 0, c_1)$ and $(c_1, 0, c_2)$, and $(c_1, 0, 0)$, respectively

B2) three saddle cycles of period 6 exist, due to the coexistence of C and the fixed point $x^\star$; they can be obtained by the periodic points $(c_1, y^\star, c_1)$ and $(c_1, y^\star, c_2)$ and $(c_1, y^\star, x^\star)$, respectively

B3) two saddle cycles of period 6 exist, due to the coexistence of C, x^* and 0. Furthermore, the two cycles can be obtained starting from the periodic points $(c_1, y^\star, 0)$ and $(c_1, 0, x^\star)$.

Fig. 4 shown two different sections of the connected component (immediate basins) of the basins of attraction of the two homogeneous stable cycles, of period 2 and of period 6. In particular we show the sections $z = c_1$ (Fig. 4.a) and $z = c_2$ (Fig. 4.b).

The boundary separating the basin of attraction $\mathcal{B}(C)$ and $\mathcal{B}(D)$ is made up by the stable sets of the three saddle cycles in

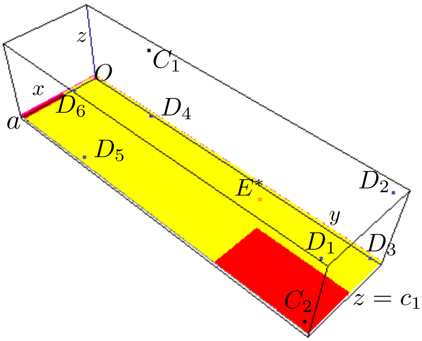

(a) Section $z = c_1$

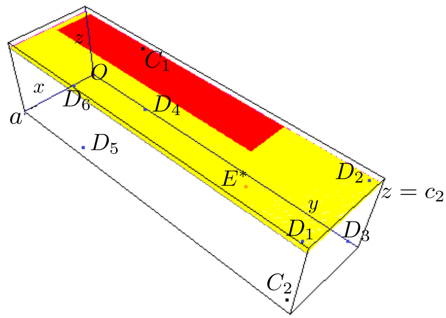

(b) Section $z = c_2$

Figure 5: Two sections of the connected component of the basins of attraction of the two coexisting cycles C and D at $k = 0.1665$

B2). On the other hand, the stable sets of the cycles in B1) and B3) bound the set of bounded trajectories, as described in the previous section (for a more accurate description of the basins of the two coexisting cycles see [3]).

3.4 Coexistence of two fixed points, a cycle of period 2 and a cycle of period 4

The number of cycles quickly becomes larger and larger when k is further decreased. For example, at $k = 0.1625$ the map H exhibits a stable cycle of period 4, born via period doubling bifurcation of $C = (c_1, c_2)$. Obviously, the appearance of such a cycle of period 4 is associated with new cycles of M, either of homogeneous or mixed type. To realize how the cardinality of the set of periodic points of M quickly increases we just consider (6). Since in the case we are considering H has 8 periodic points (2 fixed points, a cycle of period 2 and a cycle of period 4), the set $\mathcal{P}$ contains $8^3 = 512$ periodic points.

We start describing the homogeneous cycles of the map M.

From section 2.1, we obtain that M has 6 stable cycles of homogeneous type: one of period 4 and five of period 12. We can derive the periodic points of these cycles starting from the cycle $\tilde{C} = (a_1, a_2, a_3, a_4)$ of the 1D map H. The homogeneous cycle of period 4 of the map M associated with the cycle $\tilde{C}$ of H of the same period has only one periodic point with first component a_1, given by $(a_1, g(a_2), a_2)$. Regarding the cycles of period 12 of the map M, they can be obtained starting from the periodic points $(a_1, g(a_j), a_{j+1})$ with $1 \leq j \leq 2$ and $(a_1, g(a_j), a_j)$ with $1 \leq j \leq 3$.

To obtain the mixed cycles we have to consider all the possible pairs of cycles of H as well as all triplets of cycles of H containing the cycle of period 4. We have that:

- the coexistence of the cycle $\tilde{C}$ with the fixed point $x^\star$ gives rise to five saddle cycles of period 12. The periodic points of the cycles can be derived from $(a_1, g(x^\star), a_l)$, with $1 \leq l \leq 4$, and $(x_1, g(x^\star), x^\star)$;

- analogously, the coexistence of $\tilde{C}$ with the fixed point O gives rise to five saddle cycles of period 12. Their periodic points can be derived from $(a_1, 0, a_l)$, with $1 \leq l \leq 4$, and $(a_1, 0, 0)$;

- the coexistence of $\tilde{C}$ with the cycle of period 2 C gives rise to twelve saddle cycles of period 12. The periodic points of the cycles can be derived from $(a_1, g(c_j), a_l)$ and $(a_1, g(c_j), c_i)$, with $1 \leq l \leq 4$, $1 < j, i < 2$;

- the coexistence of $\tilde{C}$ with both the fixed points gives rise to two saddle cycles of period 12. The periodic points of such cycles can be derived from $(a_1, y^\star, 0)$, and $(a_1, 0, x^\star)$;

- the coexistence of $\tilde{C}$ and C with the fixed point $x^\star$ give rise to four saddle cycles of period 12. Their periodic points can be derived from $(a_1, g(c_j), x^\star)$ and $(a_1, g(x^\star), c_j)$, with $1 \leq j \leq 2$;

- analogously, the coexistence of $\tilde{C}$ and C with the fixed point O gives rise to four saddle cycles of period 12, with periodic points achievable from $(a_1, g(c_j), 0)$ and $(a_1, 0, g(c_j))$ with $1 \leq j \leq 2$.

To sum up, we can conclude that the period doubling bifurcation of the cycle 2 causes for the map M the appearance of a stable cycle of period 4, of five stable cycles of period 12 and thirty-two saddle cycles of period 12. The stable cycles are homogeneous while the saddle ones are of mixed type.

In the light of the previous analysis it can be inferred that the "*cube separate*" property enriches the dynamics of the model, allowing the coexistence of umpteen attractors.

In Fig.6 we show the six stable homogeneous cycles, one of period 4 and five of period 12 for the map M, at $k = 0.1625$. In Fig. 6 we can observe that, as expected, generally producer 1 has a higher market share, due to its more efficient production process, but there exist cycles in which producer 2 has largest production, in some phase of the cycle.

4 Chaotic attractors, chaotic surfaces and invariant curves of the map M

From the bifurcation diagram of the map H in Fig.2 we can observe the existence of chaotic attractors of the 1D map. Now, we can extend the analysis so far conducted for cycles to the case of more complex of attractors. Analogously to the cases studied above, we shall show that all the chaotic sets of the map M can be obtained as Cartesian product of the chaotic intervals of H and their conjugate, associated with the maps F and G. Then chaotic parallelepipeds are obtained in the phase space of M. To prove this fact, we extend at the three-dimension map, the results shown in [5], obtained for the two-dimension case.

Let I be any invariant set of M (i.e. $M(I) \subseteq I$) and $I_x = proj_x(I)$, $I_y = proj_y(I)$ and $I_z = proj_z(I)$, where $proj_l$ denotes

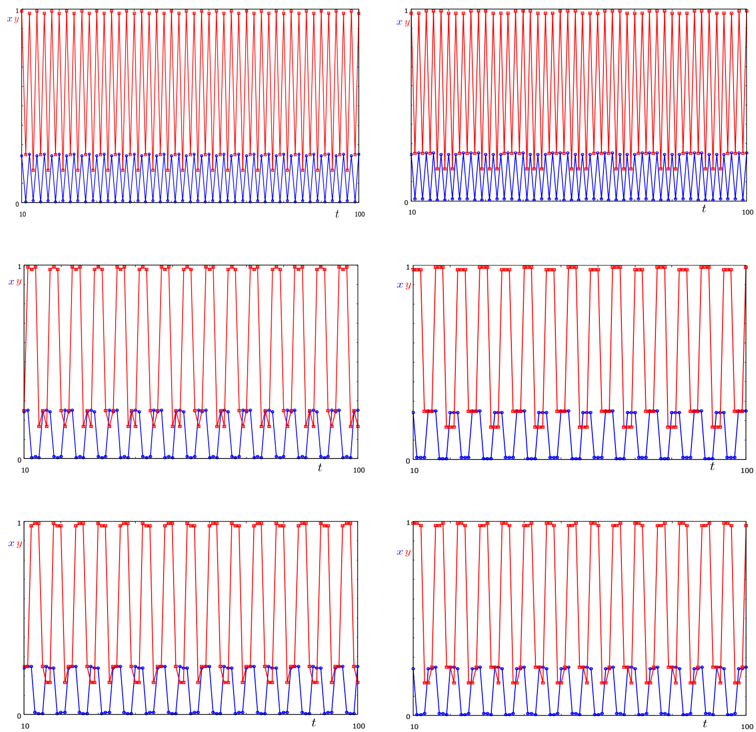

Figure 6: Coexisting stable cycles at $k = 0.1625$. Red points correspond to producer 1, while the blue ones to producers 2.

the projection onto the l-axis:

Lemma 2 *If I_x is an invariant set for $H(x) = f(g(h(x)))$ then $I_z = h(I_x)$ is invariant for $G(z) = h(f(g(z)))$ and $I_y = g(h(I_z))$ is invariant for $F(y) = g(h(f(y)))$. If I is invariant for M then its projections I_x, I_y and I_z are invariant sets for H, F and G, respectively.*

Proof. Let be I_x an invariant set of $H(x) = f(g(h(x)))$. We start proving that $I_z = h(I_x)$ is an invariant set of $G(z)$, i.e. $G(I_z) \subseteq I_z$. Let $z \in G(I_z)$, then at least one $\bar{z} \in I_z$ exists such that $G(\bar{z}) = z$, that is $h(f(g(\bar{z}))) = z$. Since $\bar{z} \in I_z = h(I_x)$, there exists at least one $\bar{x} \in I_x$ such that $h(\bar{x}) = \bar{z}$. But $G(\bar{z}) = h(f(g(\bar{z}))) = h(f(g(h(\bar{x})))) = h(H(\bar{x}))$. Then, being $H(\bar{x}) \in I_x$, we can conclude that $z = G(\bar{z}) \in h(I_x) = I_z$. Analogously we can proceed for the set I_y.

Now let I an invariant set for M and $(x, y, z) \in I$. Then $x \in I_x$, $y \in I_y$ and $z \in I_z$. We know that $M^3(x, y, z) = (H(x), F(y), G(z)) \in I$. Consequently, we obtain that $H(x) \in I_x$, $F(y) \in I_y$ and $G(z) \in I_z$, that is the projections of I are invariant sets for the associated 1D maps. ■

Lemma 3 *If I_x is an invariant set of $H(x)$ then $I_x \times I_y \times I_z$ is an invariant set of M, where $I_y = g(h(I_z))$ and $I_z = h(I_x)$.*

Proof. Let $x_0 \in I_x$, $y_0 = g(h(x_0)) \in I_y$ and $z_0 = h(x_0) \in I_z$. We have $M(x_0, y_0, z_0) = (f(g(h(x_0))), g(h(x_0)), h(x_0)) \in I_x \times I_y \times I_z$, since $f(g(h(x_0))) = H(x_0) \in I_x$. In this way we proved that $M(I_x \times I_y \times I_z) \subseteqq I_x \times I_y \times I_z$. ■

Obviously, if I_x is an invariant interval, then the associated invariant set of M (the cartesian product $I_x \times I_y \times I_z$) is a rectangular parallelepiped. In particular, in our model, the map H at $k = 0.16$ exhibits a chaotic interval I_x. Then the map M exhibits a one-piece chaotic parallelepiped given by the $I_x \times g(h(I_x)) \times h(I_x)$ (Fig.7a)

In the case in which the 1D map H has a multi-band chaotic attractor, then the same occurs for M. But, as we have seen

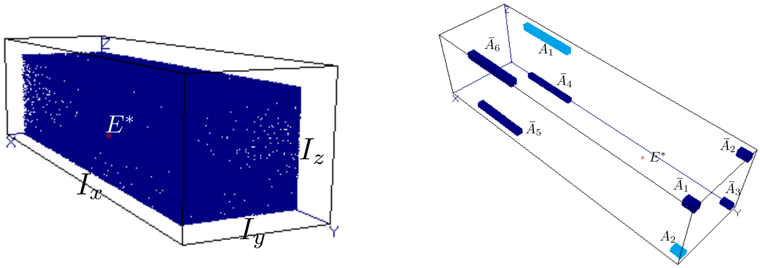

(a) $k = 0.16$. A single chaotic attractor

(b) $k = 0.161$. Two-pieces and six-pieces coexisting attractors.

Figure 7: Chaotic attractors

for cycles, the coexistence of multi-band chaotic attractors occurs, following the same rules we described in Section 3. For example, at $k = 0.161$ the map H exhibits a two-pieces chaotic attractor. This means that the map M has two coexisting attractors: a 6-pieces chaotic attractor and a 2-pieces chaotic attractor as shown in Fig.7b. To localize the two multi-pieces chaotic attractors we can proceed as in section 2.1

We have seen that if the $1D$ map H exhibits chaotic intervals, then the $3D$ map exhibits chaotic parallelepiped but, as special cases, may also exhibit chaotic surfaces and, as we shall see, even chaotic curves are possible outcome for the map M. In general we can prove the following two propositions:

Proposition 4 *Let*

$$\begin{aligned} R_1 &= \{(f(F^n(y)), y, z) : (y, z) \in I_y \times I_z\} \\ R_2 &= \{(x, g(G^n(z), z) : (x, z) \in I_x \times I_z\} \\ R_3 &= \{(x, y, h(H^n(x))) : (x, y) \in I_x \times I_y\} \end{aligned}$$

The union of the surfaces R_1, R_2, and R_3 is an invariant set of the map M, that is $M(R_1 \cup R_2 \cup R_3) \subseteq R_1 \cup R_2 \cup R_3$.

Proof. Let $(x, y, z) \in R_1$. From the property of the cycles of the $3D$ map associated with the cycles of the $1D$ maps H, F or G

(section 2.1), we obtain that

$$\begin{aligned} M\left(f\left(F^{n}\left(y\right)\right),y,z\right) &= M((H^{n}\left(f\left(y\right)\right),y,z)) \\ &= \left(f\left(y\right),g\left(z\right),h\left(f\left(F^{n}\left(y\right)\right)\right)\right) \\ &= \left(f\left(y\right),g\left(z\right),G^{n}\left(h(f\left(y\right)\right)\right) \\ &= \left(x,\bar{y},h\left(H^{n}\left(x\right)\right)\right)\in R_3 \end{aligned}$$

where $x = f(y) \in I_x$ and $\bar{y} = g(z) \in I_y$, from Proposition 1.

In a similar way we can prove that the $M(R_2) \subseteq R_1$ and $M(R_3) \subseteq R_2$. Thus, we can conclude that $M\left(R_1 \cup R_2 \cup R_3\right) \subseteq R_1 \cup R_2 \cup R_3$. ■

Proposition 5 *Let*

$$\begin{aligned} \bar{R}_1 &= \left\{\left(f\left(g\left(G^{n}\left(z\right)\right)\right),y,z\right):(y,z)\in I_y\times I_z\right\} \\ \bar{R}_2 &= \left\{\left(x,g\left(h\left(H^{n}\left(x\right)\right)\right),z\right):(x,z)\in I_x\times I_z\right\} \\ \bar{R}_3 &= \left\{\left(x,y,h\left(f\left(F^{n}\left(y\right)\right)\right)\right):(x,y)\in I_x\times I_y\right\} \end{aligned}$$

The union of the surfaces $\bar{R}_1$, $\bar{R}_2$ and $\bar{R}_3$ is an invariant set of the map M, that is $M\left(\bar{R}_1 \cup \bar{R}_2 \cup \bar{R}_3\right) \subseteq \bar{R}_1 \cup \bar{R}_2 \cup \bar{R}_3$.

Proof. Let $(x, y, z) \in \bar{R}_1$. We have that

$$\begin{aligned} M\left(f\left(g\left(G^{n}\left(x\right)\right)\right),y,z\right) &= \left(f\left(y\right),g\left(z\right),z\right) \\ &= \left(x,y,h\left(f\left(g\left(G^{n}\left(z\right)\right)\right)\right)\right) \\ &= \left(x,y,h\left(f\left(F^{n}\left(g\left(z\right)\right)\right)\right)\right) \\ &= \left(x,y,h\left(f\left(F^{n}\left(\bar{y}\right)\right)\right)\right)\in\bar{R}_3 \end{aligned}$$

where $x = f\left(y\right) \in I_x$ and $\bar{y} = g\left(z\right) \in I_y$. In similar way we can prove that $M\left(\bar{R}_2\right) \subseteq \bar{R}_1$ and $M\left(\bar{R}_3\right) \subseteq \bar{R}_2$. Thus, we can conclude that $M\left(\bar{R}_1 \cup \bar{R}_2 \cup \bar{R}_3\right) \subseteq \bar{R}_1 \cup \bar{R}_2 \cup \bar{R}_3$. ■

Recalling that the set $\left\{(x, y, z) \in \mathbb{R}^3 : z = f\left(x\right)\right\}$ is a *generalized cylinder* spanned by lines parallel to the y-axis with cross-section defined by the equations $z = f\left(x\right)$ and $y = 0$ we can say that the surfaces analyzed in the last two propositions are union of generalized cylinders.

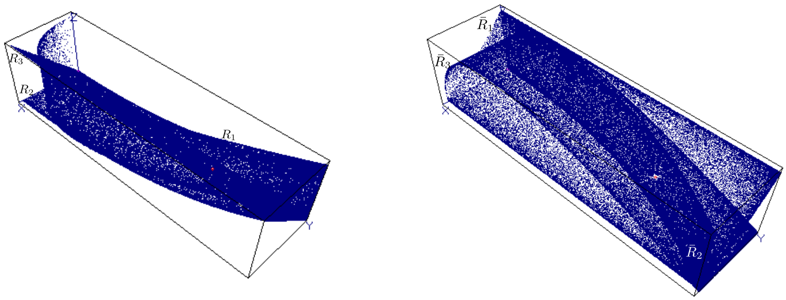

(a) ic: $(f(y_0), y_0, z_0) = (0.09, 0.01, 0.03)$ (b) ic: $(x_0, y_0, h(f(y_0))) = (0.02, 0.01, 0.09)$

Figure 8: Chaotic surfaces at $k = 0.16$

For instance, if in model (4) we consider as initial conditions

$$\begin{array}{l} (f(y_0), y_0, z_0) = (0,09; 0,01; 0,03)\ , \text{ or} \\ (x_0, y_0, h(f(y_0))) = (0,02; 0,01; 0,09) \end{array}$$

we obtain the two chaotic surfaces shown in Fig.7.

Finally, we can prove that intersecting two by two the surfaces families R_1, R_2, R_3 (or $\bar{R}_1, \bar{R}_2$, $\bar{R}_3$) we obtain an invariant set of the map M, made up by the union of three curves.

Proposition 6 *Let* $\Delta = (R_1 \cap R_2) \cup (R_2 \cap R_3) \cup (R_1 \cap R_3)$, *then*

$$M(\Delta) \subseteq \Delta$$

Proof. We consider the intersections between the surfaces R_1 and R_2, R_2 and R_3, R_1 and R_3; that is:

$$\begin{aligned} R_1 \cap R_2 &= \{(f(F^n(y)), y, z)\} \cap \{(x, g(G^n(z), z)\} \\ &= \left(H^{2n}(f(g(z))), g(G^n(z), z)\right) \\ R_2 \cap R_3 &= \{(x, g(G^n(z), z)\} \cap \{(x, y, h(H^n(x)))\} \\ &= \left(x, F^{2n}(g(h(x))), G^n(h(x))\right) \\ R_1 \cap R_3 &= \{(f(F^n(y)), y, z)\} \cap \{(x, y, h(H^n(x)))\} \\ &= \left(H^n(f(y)), y, G^{2n}(h(f(y)))\right) \end{aligned}$$

To obtain the assert, we show that $M(R_1 \cap R_2) \subseteq R_1 \cap R_3$, $M(R_1 \cap R_3) \subseteq R_2 \cap R_3$ and $M(R_2 \cap R_3) \subseteq R_1 \cap R_2$. From Proposition 2 and keeping in mind that $x \in I_x$, $y \in g(h(I_x)) = I_y$, $z \in h(I_x) = I_z$ and $g(z) = y \in I_y$ we obtain that:

$$\begin{aligned} M(R_1 \cap R_2) &= M\left(H^{2n}(f(y)), y, F^n(g(z)), z\right) = \\ &= \left(f(F^n(g(z))), g(z), h\left(H^{2n}(f(g(z)))\right)\right) = \\ &= \left(H^n(f(g(z))), g(z), G^{2n}(h(f(g(z))))\right) = \\ &= \left(H^n(f(y)), y, G^{2n}(h(f(y)))\right) \in R_1 \cap R_3 \end{aligned}$$

In similar way, we obtain:

$$\begin{aligned} M(R_2 \cap R_3) &= M\left(x, F^{2n}(g(h(x))), G^n(h(x))\right) = \\ &= \left(H^{2n}(f(g(z))), g(G^n(z), z)\right) \in R_1 \cap R_2 \end{aligned}$$

and

$$\begin{aligned} M(R_1 \cap R_3) &= M\left(H^n(f(y)), y, G^{2n}(h(f(y)))\right) = \\ &= \left(H^{2n}(f(g(z))), g(G^n(z), z)\right) \in R_1 \cap R_2 \end{aligned}$$

This allows us to conclude that $M(\Delta) \subseteq \Delta$. ■

Proposition 7 *Let* $\bar{\Delta} = (\bar{R}_1 \cap \bar{R}_2) \cup (\bar{R}_3 \cup (\bar{R}_1 \cap \bar{R}_3)$, *then*

$$M(\bar{\Delta}) \subseteq \bar{\Delta}$$

Proof. We consider the intesection between the surfaces $\bar{R}_1$ and $\bar{R}_2$. Keeping in mind that

$$\begin{aligned} g(h(H^n(f(g(G^n(z)))))) &= g(h(H^n(H^n(f(g(z)))))) \\ &= g\left(h\left(H^{2n}(f(g(z)))\right)\right) \\ &= F^{2n}(g(h(f(g(z))))) = F^{2n+1}(g(z)) \end{aligned}$$

and

$$f(g(G^n(z))) = H^n(f(g(z))),$$

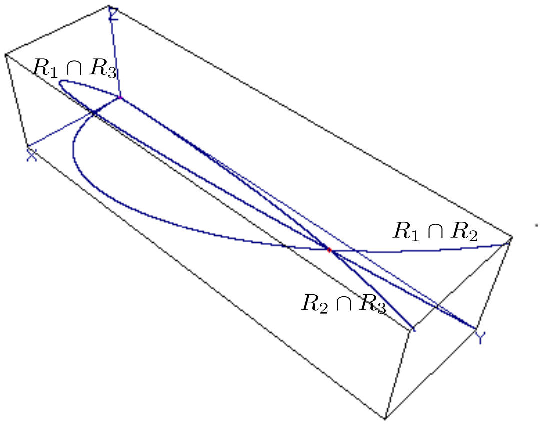

Figure 9: $k = 0.16$, ic:$(0.09, 0.01, 0.09)$. Example of a chaotic set made up by the union of three curves

we obtain that

$$\bar{R}_1 \cap \bar{R}_2 = \left\{ \left(H^n \left(f \left(g \left(z \right) \right) \right), F^{2n+1} \left(g \left(z \right) \right), z \right), z \in I_z \right\}$$

Proceeding in a similar way we get

$$\bar{R}_1 \cap \bar{R}_3 = \left\{ \left(H^{2k+1} \left(f \left(y \right) \right), y, G^k \left(h \left(f \left(y \right) \right) \right) \right), y \in I_y \right\}$$

and

$$\bar{R}_2 \cap \bar{R}_3 = \left\{ \left(x, F^n \left(g \left(h \left(x \right) \right) \right), G^{2n+1} \left(h \left(x \right) \right) \right), x \in I_x \right\}$$

To obtain the assert, as in Proposition 7, we show that

$$\begin{array}{l} M \left(\bar{R}_1 \cap \bar{R}_2 \right) \subseteq \bar{R}_1 \cap \bar{R}_3, \\ M \left(\bar{R}_1 \cap \bar{R}_3 \right) \subseteq \bar{R}_2 \cap \bar{R}_3 \text{ and} \\ M \left(\bar{R}_2 \cap \bar{R}_3 \right) \subseteq \bar{R}_1 \cap \bar{R}_2. \end{array}$$

Denoting $g(z) = \bar{y} \in I_y$, $f(y) = \bar{x} \in I_x$ and $h(x) = \bar{z} \in I_z$, we have

$$
\begin{aligned}
M\left(\bar{R}_1 \cap \bar{R}_2\right) &= \left(f\left(F^{2n+1}\left(g\left(z\right)\right)\right), g\left(z\right), h\left(H^{n}\left(f\left(g\left(z\right)\right)\right)\right)\right) = \\
&= \left(H^{2n+1}\left(f\left(g\left(z\right)\right)\right), g\left(z\right), G^{n}\left(h\left(f\left(g\left(z\right)\right)\right)\right)\right) = \\
&= \left(H^{2n+1}\left(f\left(\bar{y}\right)\right), \bar{y}, G^{n}\left(h\left(f\left(\bar{y}\right)\right)\right)\right) \in \left(\bar{R}_1 \cap \bar{R}_3\right); \\
M\left(\bar{R}_1 \cap \bar{R}_3\right) &= \left(f\left(y\right), g\left(G^{n}\left(h\left(f\left(y\right)\right)\right)\right), h\left(H^{2n+1}\left(f\left(y\right)\right)\right)\right) = \\
&= \left(\bar{x}, g\left(G^{n}\left(h\left(\bar{x}\right)\right)\right), h\left(H^{2n+1}\left(\bar{x}\right)\right)\right) = \\
&= \left(\bar{x}, F^{n}\left(g\left(h\left(\bar{x}\right)\right)\right), G^{2n+1}\left(h\left(\bar{x}\right)\right)\right) \in \left(\bar{R}_2 \cap \bar{R}_3\right); \\
M\left(\bar{R}_2 \cap \bar{R}_3\right) &= \left(f\left(F^{n}\left(g\left(h\left(x\right)\right)\right)\right), g\left(G^{2n+1}\left(h\left(x\right)\right)\right), h\left(x\right)\right) = \\
&= \left(f\left(F^{n}\left(g\left(\bar{z}\right)\right)\right), g\left(G^{2n+1}\left(\bar{z}\right)\right), \bar{z}\right) = \\
&= \left(H^{n}\left(f\left(g\left(\bar{z}\right)\right)\right), F^{2n+1}\left(g\left(\bar{z}\right)\right), \bar{z}\right) \in \left(\bar{R}_1 \cap \bar{R}_2\right)
\end{aligned}
$$

so proving the assert. ■

Fig.9 shows an example of chaotic curves for the map M.

5 Conclusion

In this paper we have studied a Cournot duopoly with isoelastic demand function and costant marginal costs. As it is well-know the reactions of the competitors are functions depending on the opponent expected production. To close the model, we have assumed that both producers have naive expectations but one of them reacts with delay to the move of its competitor.

So doing, we have obtained a discrete two-dimensional time-delayed system, ultimately described by a 3D map (map M) having third iterate with separate components. This property, that we have called "*cube separate property*" , is a extension at the three-dimensional case of the "*square separate property*" studied in [5].

Our aim was to investigate the dynamic behavior of the two firm described by the map M. In particular our study focused on the global properties of its dynamic behavior.

We have pointed out that the cube separate property causes an enrichement of the dynamics of the model allowing many situations of multistability, in which umpteen stable cycles may coexist. Characterizing the basins of attraction of different stable coexisting cycles, we have shown that, in general, they are *parallelepipeds*, separated by stable sets of saddle cycles.

Expanding the paper [4], we have also proved that, when the 1D map is chaotic, *chaotic surfaces,* having the shape of generalized cylinders, and *chaotic curves* may coexist for the map M.

References

[1] Agliari, A., Bischi, G. I., & Gardini, L. (2002). Some methods for the global analysis of dynamic games represented by iterated noninvertible maps. In Oligopoly Dynamics (pp. 31-83). Springer Berlin Heidelberg.

[2] Agliari, A., & Puu, T. (2002). A cournot duopoly with bounded inverse demand function. In Oligopoly Dynamics (pp. 171-194). Springer Berlin Heidelberg.

[3] Agliari, A. (2012, April). Coexisting cycles in a class of 3-D discrete maps. In ESAIM: Proceedings (Vol. 36, pp. 170-179). EDP Sciences.

[4] Agliari, A., Fournier-Prunaret, D., & Taha, A. K. (2013). Periodic Orbits and Their Bifurcations in 3D Maps with a Separate Third Iterate. In Global Analysis of Dynamic Models in Economics and Finance (pp. 397-427). Springer Berlin Heidelberg.

[5] Bischi, G. I., Mammana, C., & Gardini, L. (2000). Multistability and cyclic attractors in duopoly games. Chaos, Solitons & Fractals, 11(4), 543-564.

[6] Elsadany, A. A. (2010). Dynamics of a delayed duopoly game with bounded rationality. Mathematical and Computer Modelling, 52(9), 1479-1489.

[7] Elsadany, A. A., & Matouk, A. E. (2014). Dynamic Cournot Duopoly Game with Delay. Journal of Complex Systems, 2014.

[8] Gardini, L., Barugola, A., & Cathala, J. C. (1996). Chaotic dynamics in two-dimensional noninvertible maps (Vol. 20, pp. xiv+-607). Singapore: World Scientific.

[9] Gumowski, I., & Mira, C. (1980). Dynamique chaotique: transformations ponctuelles, transition ordre-désordre. Cepadues Editions.

[10] Mira, C. (1987). Chaotic dynamics. World Scientific.

[11] Mira, C., Fournier-Prunaret, D., Gardini, L., Kawakami, H., & Cathala, J. C. (1994). Basin bifurcations of two-dimensional noninvertible maps: fractalization of basins. International Journal of Bifurcation and Chaos, 4(02), 343-381.

[12] Puu, T. (1991). Chaos in duopoly pricing. Chaos, Solitons & Fractals, 1(6), 573-581.

[13] Puu, T., and I. Sushko. "Oligopoly and complex dynamics: models and tools." (2002). Springer Berlin Heidelberg new York.

[14] Yassen, M. T., & Agiza, H. N. (2003). Analysis of a duopoly game with delayed bounded rationality. Applied Mathematics and computation, 138(2), 387-402.

Printed by
Gi&Gi srl - Triuggio (MB)
July 2017

9788834334348